



HAL
open science

Uncovering the geodetic signature of silent slip through repeating earthquakes

William B. Frank, Mathilde Radiguet, Baptiste Rousset, Nikolai M. Shapiro, Allen L. Husker, Vladimir Kostoglodov, Nathalie Cotte, Michel Campillo

► **To cite this version:**

William B. Frank, Mathilde Radiguet, Baptiste Rousset, Nikolai M. Shapiro, Allen L. Husker, et al.. Uncovering the geodetic signature of silent slip through repeating earthquakes. *Geophysical Research Letters*, 2015, 42, pp.2774-2779. 10.1002/2015GL063685 . insu-03579978

HAL Id: insu-03579978

<https://insu.hal.science/insu-03579978>

Submitted on 18 Feb 2022

HAL is a multi-disciplinary open access archive for the deposit and dissemination of scientific research documents, whether they are published or not. The documents may come from teaching and research institutions in France or abroad, or from public or private research centers.

L'archive ouverte pluridisciplinaire **HAL**, est destinée au dépôt et à la diffusion de documents scientifiques de niveau recherche, publiés ou non, émanant des établissements d'enseignement et de recherche français ou étrangers, des laboratoires publics ou privés.

Copyright

RESEARCH LETTER

10.1002/2015GL063685

Key Points:

- We use repeating earthquakes as an in situ monitor of slip
- Geodetic search for slow slip guided by seismological information
- Characteristic seismic activity reveals slow slip hidden under the noise level

Supporting Information:

- Text S1 and Figure S1 caption
- Figure S1

Correspondence to:

W. B. Frank,
frank@ipgg.fr

Citation:

Frank, W. B., M. Radiguet, B. Rousset, N. M. Shapiro, A. L. Husker, V. Kostoglodov, N. Cotte, and M. Campillo (2015), Uncovering the geodetic signature of silent slip through repeating earthquakes, *Geophys. Res. Lett.*, *42*, 2774–2779, doi:10.1002/2015GL063685.

Received 1 MAR 2015

Accepted 26 MAR 2015

Accepted article online 2 APR 2015

Published online 24 APR 2015

Uncovering the geodetic signature of silent slip through repeating earthquakes

William B. Frank¹, Mathilde Radiguet², Baptiste Rousset², Nikolai M. Shapiro¹, Allen L. Husker³, Vladimir Kostoglodov³, Nathalie Cotte², and Michel Campillo²

¹Équipe de Sismologie, Institut de Physique du Globe de Paris, Paris Sorbonne Cité, CNRS, Paris, France, ²ISTerre, Université Grenoble Alpes, CNRS, IRD, Grenoble, France, ³Instituto de Geofísica, Universidad Nacional Autónoma de México, Mexico City, Mexico

Abstract Slow transient slip that releases stress along the deep roots of plate interfaces is most often observed on regional GPS networks installed at the surface. The detection of slow slip is not trivial if the dislocation along the fault at depth does not generate a geodetic signal greater than the observational noise level. Instead of the typical workflow of comparing independently gathered seismic and geodetic observations to study slow slip, we use repeating low-frequency earthquakes to reveal a previously unobserved slow slip event. By aligning GPS time series with episodes of low-frequency earthquake activity and stacking, we identify a repeating transient slip event that generates a displacement at the surface that is hidden under noise prior to stacking. Our results suggest that the geodetic investigation of transient slip guided by seismological information is essential in exploring the spectrum of fault slip.

1. Introduction

Since their discovery almost two decades ago [Linde *et al.*, 1996], slow slip events have most often been observed to release tectonic stress without measurable seismic radiation outside of the seismogenic zone at both subduction zones and transform plate interfaces [Beroza and Ide, 2011]. Slow slip can occur over several days or several months, and the slip accumulated over their duration can represent as much elastic energy release as large megathrust earthquakes ($M_w > 7$). Downdip of the seismogenic zone, the plate interface transitions from a brittle to a ductile regime due to increasing temperatures and pressures along with higher pore fluid pressure resulting from metamorphic dehydration reactions of the subducting slab, facilitating the generation of silent or slow slip [Audet *et al.*, 2009; Song *et al.*, 2009; Peacock *et al.*, 2011; Audet and Bürgmann, 2014]. Slow slip is most often detected as transient displacements observed at continuous GPS (cGPS) stations [Hirose *et al.*, 1999; Dragert *et al.*, 2001; Kostoglodov *et al.*, 2003]; any silent slip at depth that does not generate sufficient displacement at the surface will therefore most likely not be observed on GPS time series. By exploiting the repeating nature of low-frequency earthquakes [e.g., Shelly *et al.*, 2006], small shearing events along the plate interface that are strongly correlated with slow slip [Frank *et al.*, 2014], we are able to lower the geodetic noise level to reveal recurring transient slip events.

2. Low-Frequency Earthquakes in Guerrero, Mexico

We study here the Guerrero segment of the Mexican subduction zone (Figure 1) where large ($M_w > 7.5$) slow slip events occur about every 4 years and are accompanied by tectonic tremor and low-frequency earthquakes, seismic phenomena coincident with silent slip along the plate interface [Kostoglodov *et al.*, 2010; Husker *et al.*, 2012; Radiguet *et al.*, 2012; Frank *et al.*, 2013, 2014]. A dense, linear seismic network [MASE, 2007] that was installed from Acapulco up to Tampico and going through Mexico City continuously recorded for 2.5 years, notably during the M_w 7.5 2006 slow slip event that lasted 6 months from April to November [Radiguet *et al.*, 2011]. This data set has been mined with systematic detection algorithms, producing a very dense low-frequency earthquake catalog in both time and space with almost 2 million events spread over 1120 unique sources [Frank and Shapiro, 2014; Frank *et al.*, 2014]. Given that each low-frequency earthquake source will repeatedly produce events at rates that correlate in time with slow slip, we use their rates of activity as an in situ probe to monitor the fault conditions at the subduction interface [Frank *et al.*, 2014, 2015].

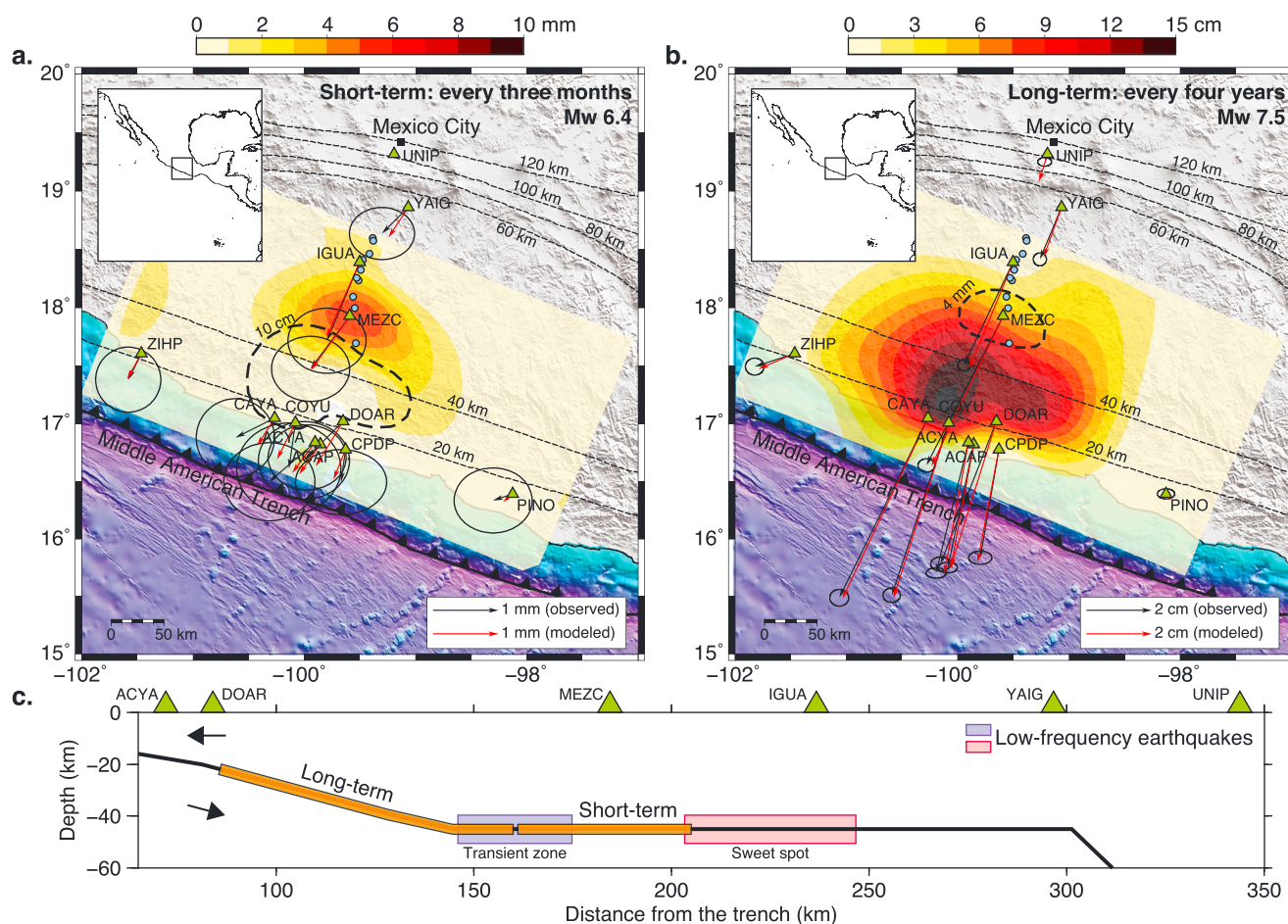


Figure 1. Slow slip in the Guerrero subduction zone. The geometry of the plate interface is shown by the thin dashed black depth contours [Kim *et al.*, 2013]. Local cGPS and seismic stations are represented, respectively, by green triangles and blue circles. The observed displacement vectors (black) for both the averaged (a) short-term slow slip and the (b) long-term 2006 slow slip are plotted with 1σ error ellipses. The slip distribution at the plate interface from the static inversion of the observed displacements is shown for both cycles of slow slip; the corresponding displacement vectors at the surface are shown in red. The thick dashed black contours indicate the main concentration of slip along the plate interface during the other slow slip cycle. (c) The two low-frequency earthquake source regions are shown by the colored boxes. The segments of the plate interface that correspond to the slip contours in Figures 1a and 1b are outlined by the orange rectangles. The black arrows show the gross tectonic movement during slow slip in Guerrero.

The Guerrero low-frequency earthquakes are distributed into two source regions along the plate interface (Figure 1c) that have distinctly different activity regimes [Frank *et al.*, 2014]. The sweet spot, located the farthest downdip, emits bursts of low-frequency earthquakes in an almost continuous fashion, indicating a near-constant accommodation of tectonic stress and therefore a slip regime at the interface that is closer to stable sliding [Husker *et al.*, 2012; Frank *et al.*, 2013]. Farther updip in the transient zone, low-frequency earthquake activity is distributed into distinct episodes as shown in Figure 2, the largest of which occurs during the 2006 slow slip event [Frank *et al.*, 2014]. Given that the majority of activity within the transient zone occurs during a large slow slip event, we explore in the following the feasibility of each of the low-frequency earthquake episodes outside of the large 2006 event representing a smaller short-term slow slip. Previous studies [Vergnolle *et al.*, 2010; Husker *et al.*, 2012; Zigone *et al.*, 2012; Rivet *et al.*, 2014] have suggested the same possibility, but the geodetic signature of such small slip events has yet to be confirmed on the local cGPS network due to low signal-to-noise ratios (Figure 1).

2.1. Characteristic Low-Frequency Earthquake Episodes

We identify seven low-frequency earthquake episodes (Figure 2) within the Guerrero catalog that each have several characteristic features [cf. Frank *et al.*, 2014, Figure 7]. At the start of each episode, low-frequency earthquakes are first observed in the most downdip portion of the sweet spot and then migrate updip farther into the sweet spot. This is then followed by a number of streaking migrations over 3 to 4 days that travel at about

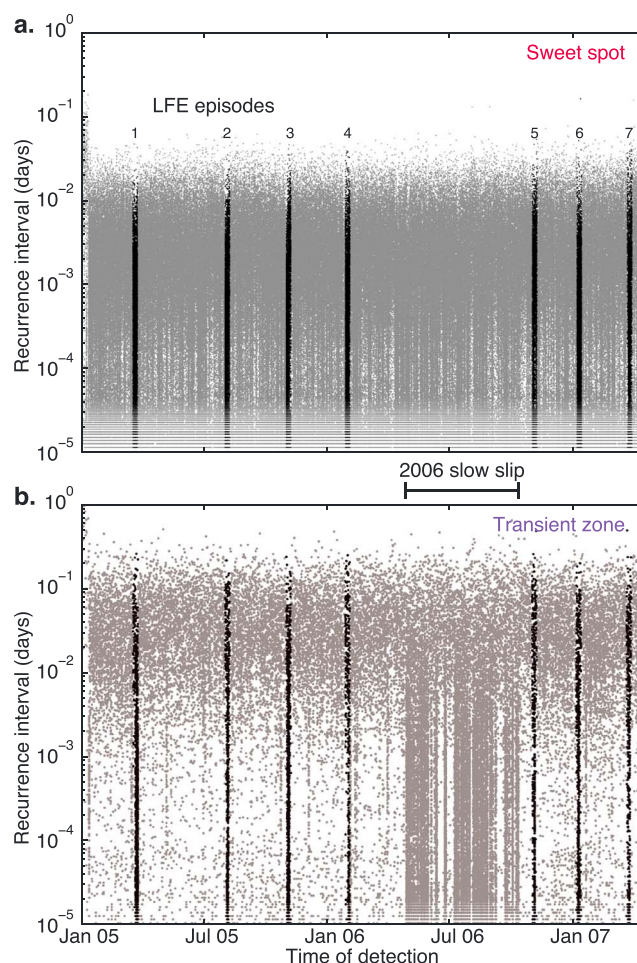


Figure 2. Low-frequency earthquake catalog in Guerrero, Mexico. The plotted recurrence intervals for each event are defined as the elapsed time between sequential low-frequency earthquakes in a given source region, (a) the sweet spot or (b) the transient zone. The seven identified low-frequency earthquake episodes are indicated in Figure 2a. All low-frequency earthquakes observed during the episodes are drawn as black points; every other low-frequency earthquake in the Guerrero catalog is shown as a grey point. The transient zone emits the highest rates of low-frequency earthquakes during the large 2006 slow slip and the identified episodes.

seven episodes by the maximum of the cross correlations of the detrended counts in the transient zone because activity there is more punctual than in the sweet spot due to its more brittle stick-slip activity regime [Frank et al., 2015]. We prepare the GPS time series in a similar manner by applying 300 day windows to each of the seven episodes and removing the secular or linear interslow slip trend at each of the cGPS stations (except for UNIP which did not function before 2006), determined as the displacement rate before the large 2006 slow slip event. With each of the episodes well aligned relative to one another using low-frequency earthquakes as a guide, we now stack the GPS time series.

Figure 3a presents the south-north displacement time series on the regional cGPS network alongside the detrended low-frequency earthquake activity stacked over the seven identified episodes. We observe a clear maximum displacement of about 1.5 mm toward the south on the stacked displacement time series at both cGPS stations closest to the transient zone, MEZC and IGUA. This movement is consistent with a release of tectonic stress but is at least 20 times smaller than the 4–5 cm displacements observed at the same stations during the larger 2006 slow slip event. This displacement is not visible on the individual GPS time series, but a coherent signal across the entire regional GPS network emerges after stacking as shown in Figures 3b and

25 km h⁻¹ in both updip and downdip directions but are constrained to the sweet spot. Activity then finally breaks into the transient zone and lasts for 2 to 3 days; no streaking migrations are observed, but this is most likely due to the sparse density of low-frequency earthquake sources in the transient zone. The total duration of any episode is never longer than 7 days. Given the similar time-space history of each episode, we propose that each low-frequency earthquake episode represents a repeating transient slip event.

3. Low-Frequency Earthquake Episodes as Repeating Slip

To test whether this supposition is true, we use the identified episodes as a guide to stack the GPS time series. If each low-frequency earthquake episode represents a recurring slow slip event, we suppose that any coherent signal in the GPS time series will constructively stack, while the random noise will sum incoherently. We determine the timing of each episode in Figure 2 by picking the highest rate of low-frequency earthquakes during each episode. Low-frequency earthquake activity during each picked episode is represented by their detrended cumulative event count (Figure 3). We determine this quantity by calculating the cumulative low-frequency earthquake count during a 300 day window centered on each of our manual episode picks and removing the best fit linear trend. Individual detrended counts are calculated for both the transient zone and the sweet spot. To refine our picks of the episodes, we align the

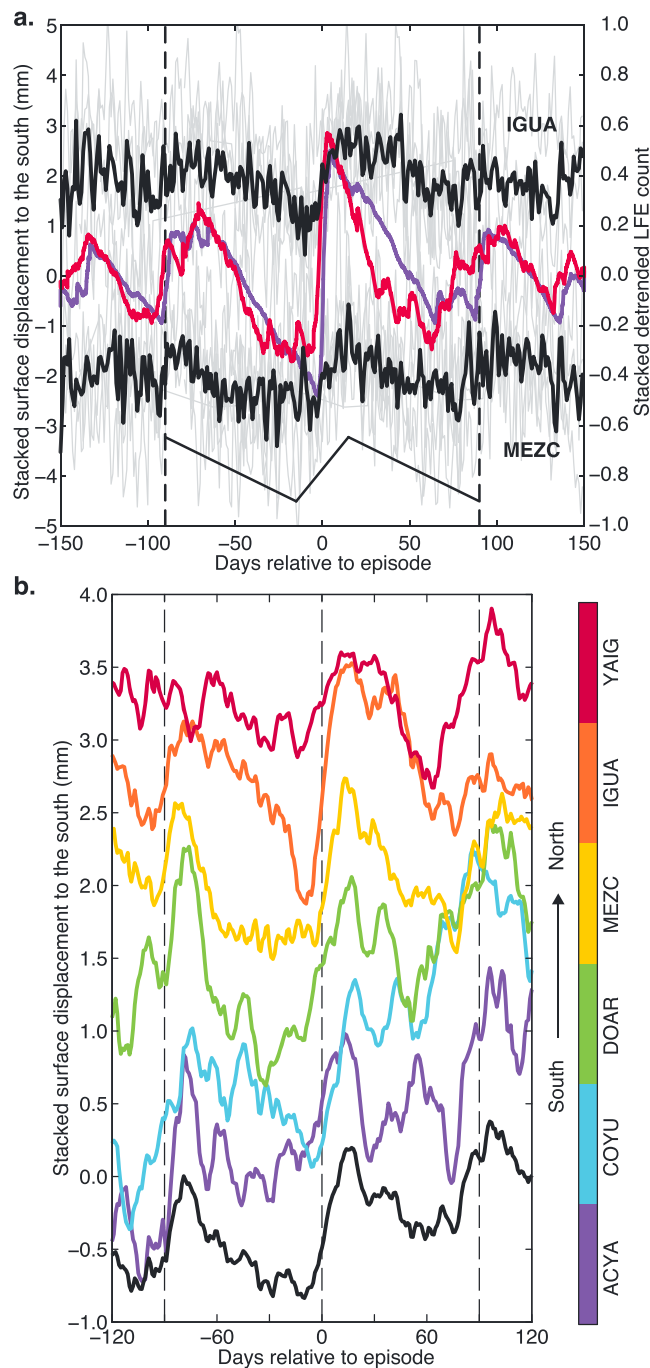


Figure 3. Stacked south-north GPS time series and low-frequency earthquake (LFE) activity trends. (a) After the noisy individual time series (gray lines) centered on each episode at the two closest cGPS stations are stacked (black lines), a southward displacement of about 1.5 mm is visible at 0 and ± 90 days (dashed lines), evidence of a periodic short-term slow slip event. The stacked detrended cumulative LFE counts of the transient zone (purple) and the sweet spot (red) also constructively stack at 0 and ± 90 days, confirming that the entire LFE source region activates during smaller slow slip just as it does for the large slow slip events. (b) The recurring short-term slow slip is visible across the entire network as evidenced by the stacked 10 day smoothed south-north displacement time series (colored lines). The average stacked displacement for the plotted subset of stations is shown in black.

S1 in the supporting information. We suggest that the coherent movement at day 0 on the stacked GPS time series represents the displacement resulting from an “averaged” slow slip event over the seven individual episodes. In addition to the primary displacement during the episodes, we observe smaller movements to the south at about ± 90 days relative to the episode that are also accompanied by low-frequency earthquake activity. We suggest that these smaller displacements indicate a 3 month periodicity of the short-term slow slip events. To compare, the mean recurrence of the seven low-frequency earthquake episodes is 91 days. A variability in the 90 day periodicity and the averaging in time and space over seven different events most likely causes smearing during the stacking process and explains the relatively smaller displacements at ± 90 days. That this signal only emerges after stacking suggests that this slow slip cycle was previously hidden within the noise and explains why it was not previously observed. The coherent displacement across the network along with the observed periodicity confirms that each episode represents a recurring short-term release of tectonic stress whose slip distribution is similar over each of the seven episodes.

3.1. Comparing Short- and Long-Term Slow Slip

To estimate the amount of dislocation at the plate interface during this averaged short-term slow slip event, we pick the displacement vectors for each of the local cGPS stations on the stacked GPS time series. We estimate the error of our picks as the standard deviation of the stacked 300 day window. A qualitative comparison between the displacement vectors of the short-term slow slip (Figure 1a) with those of the 2006 event (Figure 1b) shows that the inland displacements are relatively larger than the coastal displacements, suggesting a different slip distribution at the plate interface. To better constrain the source region of the averaged short-term slow slip, we perform a static inversion of the slip that we further detail in the supporting information. We present the final slip distributions for both the small and large slow slip events [Radiguet *et al.*, 2011] in Figure 1. The maximum slip of 6 mm of the averaged slow slip is significantly smaller than the 16 cm of slip estimated for the large 2006 slow slip event but comparable to the faster slow slip events around the world, such as the 2 cm events that occur every 14 months in Cascadia [Dragert *et al.*, 2001] or the 1.2 cm events that occur every 6 months in central Japan [Hirose and Obara, 2006]. We consider the modeled short-term slow slip magnitude of M_w 6.4 as an upper limit due to the strong smoothing applied to take into account the uncertainties of the measured displacements.

The greatest concentration of slip for the small events is located between the transient zone and the sweet spot, farther downdip than the location of maximum slip for the large slow slip events. Along with the observed relatively larger displacements inland, this further suggests that a different portion of the subduction interface slips during the small and large events. Just as the recurrence times of tectonic tremor and low-frequency earthquakes are observed to decrease with distance from the trench due to the changing frictional properties along the subduction interface [Obara *et al.*, 2010; Wech and Creager, 2011; Frank *et al.*, 2015], we suggest that there are multiple slow slip cycles along dip and that there is an analogous decrease of recurrence for slow slip events with distance from the trench. These observations along with others [Hirose and Obara, 2005; Obara, 2011] corroborate a recent suggestion that there is a continuum of slip modes that correspond to the full spectrum of possible friction regimes between stick-slip and stable sliding [Peng and Gomberg, 2010; Wech and Creager, 2011]. There are several proposed models that can explain the decreasing recurrence intervals with increasing distance from the trench, such as a temperature-controlled evolution of friction [Wech and Creager, 2011] or a progressive enrichment and deposition of silica along the subduction interface that lowers permeability and favors the development of high pore fluid pressure [Audet and Bürgmann, 2014]. Given that temperatures at the interface still increase along dip despite a subhorizontal subduction interface [Manea and Manea, 2011], both models, being primarily temperature controlled, are feasible and it is not possible for us to favor one model or the other based on our observations. Regardless of the model, pore fluid pressure is very likely to play a significant role in Guerrero [Manea and Manea, 2011; Frank *et al.*, 2015].

4. Conclusions

Using low-frequency earthquakes in Guerrero, Mexico as an in situ monitor of where and when slow slip is occurring on the subduction interface, we have presented an example of how systematically cataloged seismic repeater activity can be used to lower the noise level of cGPS stations and detect small amplitude slip transients. Although we focus on cGPS data in this study, the same principle of detecting new small transient slips through seismic observations applies to other types of geodetic instruments, such as strainmeters and

tiltmeters. We speculate that through the systematic cataloging and analysis of repeating earthquakes, seismologically guided geodetic observations will become an important tool in revealing previously unobserved slip modes at other plate interfaces around the world and understanding how and where slip occurs.

Acknowledgments

Analyzed GPS time series and low-frequency earthquake catalog is available upon request to the corresponding author. We thank Caltech for providing the analyzed Meso-America Subduction Experiment data set and the SSN and INEGI for making the GPS data set available. This work was supported by the Agence Nationale de la Recherche (France) under the contract RA000CO69 (G-GAP), the DataScale project and Labex OSUG@2020 (Investissements d'avenir ANR10 LABX56), by the European Research Council under the contract FP7 ERC Advanced grant 227507 (WHISPER), by PAPIIT IN110514 and CONACYT 178058 (Mexico), and by the Russian Science Foundation (grant 14-47-00002). Numerical computations were performed on the S-CAPAD platform, IPGP, France.

The Editor thanks Pascal Audet and Joan Gomberg for their assistance in evaluating this paper.

References

- Audet, P., and R. Bürgmann (2014), Possible control of subduction zone slow-earthquake periodicity by silica enrichment, *Nature*, *510*, 389–392, doi:10.1038/nature13391.
- Audet, P., M. G. Bostock, N. I. Christensen, and S. M. Peacock (2009), Seismic evidence for overpressured subducted oceanic crust and megathrust fault sealing, *Nature*, *457*, 76–78, doi:10.1038/nature07650.
- Beroza, G. C., and S. Ide (2011), Slow earthquakes and nonvolcanic tremor, *Annu. Rev. Earth Planet. Sci.*, *39*, 271–296, doi:10.1146/annurev-earth-040809-152531.
- Dragert, H., K. Wang, and T. S. James (2001), A silent slip event on the deeper Cascadia subduction interface, *Science*, *292*, 1525–1528, doi:10.1126/science.1060152.
- Frank, W. B., and N. M. Shapiro (2014), Automatic detection of low-frequency earthquakes (LFEs) based on a beamformed network response, *Geophys. J. Int.*, *197*(2), 1215–1223, doi:10.1093/gji/ggu058.
- Frank, W. B., N. M. Shapiro, V. Kostoglodov, A. L. Husker, M. Campillo, J. S. Payero, and G. A. Prieto (2013), Low-frequency earthquakes in the Mexican sweet spot, *Geophys. Res. Lett.*, *40*, 2661–2666, doi:10.1002/grl.50561.
- Frank, W. B., N. M. Shapiro, A. L. Husker, V. Kostoglodov, A. Romanenko, and M. Campillo (2014), Using systematically characterized low-frequency earthquakes as a fault probe in Guerrero, Mexico, *J. Geophys. Res. Solid Earth*, *119*, 7686–7700, doi:10.1002/2014JB011457.
- Frank, W. B., N. M. Shapiro, A. L. Husker, V. Kostoglodov, H. S. Bhat, and M. Campillo (2015), Along-fault pore-pressure evolution during a slow-slip event in Guerrero, Mexico, *Earth Planet. Sci. Lett.*, *413*, 135–143, doi:10.1016/j.epsl.2014.12.051.
- Hirose, H., and K. Obara (2005), Repeating short- and long-term slow slip events with deep tremor activity around the Bungo channel region, southwest Japan, *Earth Planets Space*, *57*(10), 961–972.
- Hirose, H., and K. Obara (2006), Short-term slow slip and correlated tremor episodes in the Tokai region, central Japan, *Geophys. Res. Lett.*, *33*, L17311, doi:10.1029/2006GL026579.
- Hirose, H., K. Hirahara, F. Kimata, N. Fujii, and S. Miyazaki (1999), A slow thrust slip event following the two 1996 Hyuganada earthquakes beneath the Bungo Channel, southwest Japan, *Geophys. Res. Lett.*, *26*(21), 3237–3240, doi:10.1029/1999GL010999.
- Husker, A. L., V. Kostoglodov, V. M. Cruz-Atienza, D. Legrand, N. M. Shapiro, J. S. Payero, M. Campillo, and E. Huesca-Pérez (2012), Temporal variations of non-volcanic tremor (NVT) locations in the Mexican subduction zone: Finding the NVT sweet spot, *Geochem. Geophys. Geosyst.*, *13*, Q03011, doi:10.1029/2011GC003916.
- Kim, Y., R. W. Clayton, P. D. Asimow, and J. M. Jackson (2013), Generation of talc in the mantle wedge and its role in subduction dynamics in central Mexico, *Earth Planet. Sci. Lett.*, *384*, 81–87, doi:10.1016/j.epsl.2013.10.006.
- Kostoglodov, V., S. K. Singh, J. A. Santiago, S. I. Franco-Sanchez, K. M. Larson, A. R. Lowry, and R. G. Bilham (2003), A large silent earthquake in the Guerrero seismic gap, Mexico, *Geophys. Res. Lett.*, *30*(15), 1807, doi:10.1029/2003GL017219.
- Kostoglodov, V., A. L. Husker, N. M. Shapiro, J. S. Payero, M. Campillo, N. Cotte, and R. W. Clayton (2010), The 2006 slow slip event and nonvolcanic tremor in the Mexican subduction zone, *Geophys. Res. Lett.*, *37*, L24301, doi:10.1029/2010GL045424.
- Linde, A. T., M. T. Gladwin, M. J. S. Johnston, R. L. Gwyther, and R. G. Bilham (1996), A slow earthquake sequence on the San Andreas Fault, *Nature*, *383*, 65–68.
- Manea, V. C., and M. Manea (2011), Flat-slab thermal evolution structure and evolution beneath Central Mexico, *Pure Appl. Geophys.*, *168*, 1475–1487.
- MASE (2007), Meso America Subduction Experiment, Caltech, Dataset, doi:10.7909/C3RN355P.
- Obara, K. (2011), Characteristics and interactions between non-volcanic tremor and related slow earthquakes in the Nankai subduction zone, southwest Japan, *J. Geodyn.*, *52*(3–4), 229–248, doi:10.1016/j.jjog.2011.04.002.
- Obara, K., S. Tanaka, T. Maeda, and T. Matsuzawa (2010), Depth-dependent activity of non-volcanic tremor in southwest Japan, *Geophys. Res. Lett.*, *37*, L13306, doi:10.1029/2010GL043679.
- Peacock, S. M., N. I. Christensen, M. G. Bostock, and P. Audet (2011), High pore pressures and porosity at 35 km depth in the Cascadia subduction zone, *Geology*, *39*(5), 471–474, doi:10.1130/G31649.1.
- Peng, Z., and J. S. Gomberg (2010), An integrated perspective of the continuum between earthquakes and slow-slip phenomena, *Nat. Geosci.*, *3*, 599–607, doi:10.1038/ngeo940.
- Radiguet, M., F. Cotton, M. Vergnolle, M. Campillo, B. Valette, V. Kostoglodov, and N. Cotte (2011), Spatial and temporal evolution of a long term slow slip event: The 2006 Guerrero slow slip event, *Geophys. J. Int.*, *184*(2), 816–828, doi:10.1111/j.1365-246X.2010.04866.x.
- Radiguet, M., F. Cotton, M. Vergnolle, M. Campillo, A. Walpersdorf, N. Cotte, and V. Kostoglodov (2012), Slow slip events and strain accumulation in the Guerrero gap, Mexico, *J. Geophys. Res.*, *117*, B04305, doi:10.1029/2011JB008801.
- Rivet, D., et al. (2014), Seismic velocity changes, strain rate and non-volcanic tremors during the 2009–2010 slow slip event in Guerrero, Mexico, *Geophys. J. Int.*, *196*, 447–460, doi:10.1093/gji/ggt374.
- Shelly, D. R., G. C. Beroza, S. Ide, and S. Nakamura (2006), Low-frequency earthquakes in Shikoku, Japan, and their relationship to episodic tremor and slip, *Nature*, *442*, 188–191, doi:10.1038/nature04931.
- Song, T.-R. A., D. V. HelMBERGER, M. R. Brudzinski, R. W. Clayton, P. M. Davis, X. Pérez-Campos, and S. K. Singh (2009), Subducting slab ultra-slow velocity layer coincident with silent earthquakes in southern Mexico, *Science*, *324*, 502–506, doi:10.1126/science.1167595.
- Vergnolle, M., A. Walpersdorf, V. Kostoglodov, P. Tregoning, J. A. Santiago, N. Cotte, and S. I. Franco-Sanchez (2010), Slow slip events in Mexico revised from the processing of 11 year GPS observations, *J. Geophys. Res.*, *115*, B08403, doi:10.1029/2009JB006852.
- Wech, A. G., and K. C. Creager (2011), A continuum of stress, strength and slip in the Cascadia subduction zone, *Nat. Geosci.*, *4*, 624–628, doi:10.1038/ngeo1215.
- Zigone, D., D. Rivet, M. Radiguet, M. Campillo, C. Voisin, N. Cotte, A. Walpersdorf, N. M. Shapiro, G. Cougoulat, and P. Roux (2012), Triggering of tremors and slow slip event in Guerrero, Mexico, by the 2010 Mw 8.8 Maule, Chile, earthquake, *J. Geophys. Res.*, *117*, B09304, doi:10.1029/2012JB009160.